



# Journal of Geophysical Research: Biogeosciences

## RESEARCH ARTICLE

10.1002/2016JG003572

#### **Key Points:**

- Particulate organic P remineralization is a significant source of dissolved P in the water column of the Chesapeake Bay
- The composition and transformation of particulate organic P responds strongly to seasonal and redox conditions
- Authigenic precipitation of calcium phosphate is speculated in the P-rich hypoxic water column

### Supporting Information:

Supporting Information S1

Correspondence to: D. P. Jaisi, iaisi@udel.edu

#### Citation:

Li, J., P. Reardon, J. P. McKinley, S. R. Joshi, Y. Bai, K. Bear, and D. P. Jaisi (2017), Water column particulate matter: A key contributor to phosphorus regeneration in a coastal eutrophic environment, the Chesapeake Bay, J. Geophys. Res. Biogeosci., 122, doi:10.1002/2016JG003572.

Received 3 AUG 2016 Accepted 6 MAR 2017 Accepted article online 8 MAR 2017

# Water column particulate matter: A key contributor to phosphorus regeneration in a coastal eutrophic environment, the Chesapeake Bay

Jiying Li<sup>1</sup> , Patrick Reardon<sup>2,3</sup> , James P. McKinley<sup>4</sup> , Sunendra R. Joshi<sup>1</sup> , Yuge Bai<sup>1</sup>, Kristi Bear<sup>1</sup>, and Deb P. Jaisi<sup>1</sup>

<sup>1</sup> Department of Plant and Soil Sciences, University of Delaware, Newark, Delaware, USA, <sup>2</sup>Environmental Molecular Sciences Laboratory, Pacific Northwest National Laboratory, Richland, Washington, USA, <sup>3</sup>Now at NMR Facility, Oregon State University, Corvallis, Oregon, USA, <sup>4</sup>Geochemistry Group, Pacific Northwest National Laboratory, Richland, Washington, USA

Abstract Particulate phosphorus (PP) in the water column is an essential component of phosphorus (P) cycling in the Chesapeake Bay because P often limits primary productivity, yet its composition and transformation remain undercharacterized. To understand the mobilization of PP and P sequestration in the water column, we studied seasonal variations in particulate organic and inorganic P species at three sites in the Chesapeake Bay, using chemical extractions, 1-D (31P) and 2-D (1H-31P) NMR spectroscopies, and electron microprobe analyses. Our results suggest that an average of 9% and 50% of water column PP was recycled in shallow and deep sites, respectively, primarily through remineralization of organic P, which was 3 times higher than Fe-bound P remobilization. P recycling efficiency was highest in the warm and anoxic seasons. Organic P compositions and concentrations responded strongly to seasonal and redox variations: orthophosphate monoesters and diesters, and diester-to-monoester ratios (D/M) decreased with depth; both esters and D/M ratios were lower in the anoxic waters in July and September. In contrast, pyrophosphate concentration increased with depth and polyphosphate concentration was high in anoxic seasons. Our analyses suggest the presence of Ca-phosphate minerals (Ca-P) in the water column but with concentrations comparable to sediment Ca-P. It is unclear, however, whether authigenic precipitation occurred in the water column or resuspended from sediments. Overall, these results reveal the dominance of internal P cycling particularly via organic P remineralization and controlling P availability in the water column of the Chesapeake Bay.

## 1. Introduction

Phosphorus (P) is frequently the limiting nutrient in aquatic ecosystems that controls primary productivity and determines trophic states [Hecky and Kilham, 1988; Karl, 2014]. The Chesapeake Bay, the largest estuary in the United States, has been suffering from summer eutrophication and hypoxia for several decades [Cornwell et al., 1996; Hagy et al., 2004; Kemp et al., 2005]. The high dissolved inorganic nitrogen to phosphorus ratios (> Redfield ratio) in the upper Bay and in early seasons (spring to summer) suggests that P often limits primary productivity [Fisher et al., 1999; Kemp et al., 2005; Prasad et al., 2010]. Water quality restoration in the Bay is complicated by the temporally and spatially variable nutrient sources [Ator and Denver, 2015]. Within the many external P inputs (such as river runoff, atmospheric deposition, point discharges, and submarine discharge), particulate P is the major P input form [Biggs, 1970; Boynton et al., 1995; Conley et al., 1995; Keefe, 1994]. Remobilization of particular inorganic P phases (most importantly P-bearing Fe-(oxyhydr)oxides; Fe-P hereafter) in the water column, especially in hypoxic seasons, may release a significant amount of dissolved P, the preferred P form for primary productivity [Boynton et al., 1995; Conley et al., 1995; Fitzsimons et al., 2012]. As is the case for many aquatic ecosystems, internal P supply via degradation of organic matter from primary production is also an essential contributor to bioavailable P in the water column [Boynton et al., 1995; Hupfer et al., 1995; Cowan and Boynton, 1996]. On the other hand, P sequestration in the water column (e.g., via authigenic precipitation of less reactive minerals) is also a key component in P cycling, as the sinking particulates ultimately reach sediments and become a long-term P sink [Faul et al., 2005; Hyacinthe and Van Cappellen, 2004; Jilbert and Slomp, 2013; Lyons et al., 2011]. Understanding the relative importance of the major sources/pathways (Fe oxide-bound P remobilization versus organic P remineralization) and sinks of bioavailable P and their spatial and temporal variations is crucial for nutrient management.

©2017. American Geophysical Union. All Rights Reserved.



In contrast to the sediments where P speciation, transformations, and effluxes across the sediment-water interface have been extensively studied and models developed [e.g., Boynton and Kemp, 1985; Boynton and Bailey, 2008; Cowan and Boynton, 1996; Joshi et al., 2015; Wang et al., 2003], the settling particulates in the Bay water column remain largely uncharacterized [Conley et al., 1995]. Knowledge is scarce about water column particulate P, not only in the Chesapeake Bay but also in other water bodies, in regard to their compositions (organic and inorganic P phases), cycling (remineralization and remobilization), and sequestration processes, as well as their environmental controls such as temperature, salinity, and redox conditions [Paytan et al., 2003; Read et al., 2014; Schenau et al., 2000; Sannigrahi and Ingall, 2005; Sekula-Wood et al., 2012]. The strong spatial and seasonal variability in the Bay provides an excellent opportunity to investigate the mechanistic controls of water column particulate P transformation in similar eutrophic systems.

This paper investigates the role of water column particulates in P cycling in the Chesapeake Bay. Here we present results from a 2 year, multiseasonal investigation of the particulate P at three locations along the salinity gradient in the Bay. We characterize the particulate P species in the water column of the Bay using chemical extractions, solution 1-D (<sup>31</sup>P) and 2-D (<sup>1</sup>H-<sup>31</sup>P) NMR, and electron microprobe analysis (EMPA) with an aim to understand the forms and transformations of settling particulate P—remineralization of organic P, remobilization of Fe-P, and precipitation of authigenic Ca-P—as well as to identify their controlling factors.

### 2. Materials and Methods

## 2.1. Sample Collection and Physicochemical Characterization

Water and suspended particle samples were collected in the water column at three locations (sites 1.1, 3.3C, and 5.2) along the main stem of the Chesapeake Bay in multiple seasons aboard the R/V Kerhin in 2014–2015 (Figure 1a and Table 1). The sampling seasons (spring to early fall) covered the period of hypoxia development in the Chesapeake Bay. The sampling sites were the same as those of the Tidal Main Stem Water Quality Monitoring Project conducted by the Chesapeake Bay Program [2016], where water quality data are available since 1984 (http://data.chesapeakebay.net/WaterQuality). The freshwater site 1.1 is located at the mouth of Susquehanna River, whereas sites 3.3C and 5.2 are located in the mesohaline region downstream from the turbidity maximum near the Bay bridge and mouth of the Potomac River, respectively (Figure 1a). Sites 3.3C and 5.2 are located in the region of the highest productivity [Zhang et al., 2006] but site 3.3C typically experiences the most intense eutrophication and longest summer hypoxia.

Water temperature, dissolved oxygen, pH, and salinity were measured in situ using a Hydrolab probe (Hydrolab Surveyor II) attached to a sampling pump. Water samples were analyzed by the CBP for total suspended particles (TSS), particulate phosphorus (PP), total dissolved phosphorus (TDP), dissolved soluble reactive phosphorus (SRP, mostly inorganic P, therefore DIP is used hereafter), ammonium, chlorophyll *a*, and pheophytin concentrations (for detailed description of the methods see *Chesapeake Bay Program*, [2012]). In brief, water samples for these analyses were filtered in the field using 0.7 µm Whartman GF/F filters and a vacuum pump to separate dissolved and solid substances (0.7 µm filter was chosen to avoid dogging, and a study showed that the difference was insignificant between using 0.45 and 0.7 µm filters [*Chesapeake Bay Program*, 2012]. Particulate P concentrations were measured following the method of *Aspila et al*. [1976]. DIP was measured using the molybdenum blue method (EPA method 365). Total dissolved P (TDP) was determined by digesting samples in acid and persulfate to convert all forms of dissolved P to inorganic orthophosphate. Dissolved organic phosphorus (DOP) was calculated by subtracting DIP from TDP.

Separate particulate samples were collected to characterize P speciation. Suspended particles were collected within  $\sim$  24–40 L of water for selected depth intervals (Table 1): surface (S; 0.5 m), above pycnocline (AP), below pycnocline (BP), and bottom (B; 0.5 m above the sediment-water interface). Samples were stored on ice in coolers immediately after collection and were processed upon arriving at the laboratory at the University of Delaware. Suspended particles were separated from the water samples using centrifugation (Sorvall LYNX 6000), and Stokes' law of settling was applied to obtain particulate P with > 0.1  $\mu$ m particle size. Collected particles were lyophilized and homogenized prior to analyses. Some degree of oxidation for anoxic samples may have occurred during sample handling which may have caused some artifacts (e.g., overestimation of ferric Fe-P, although this is not likely to be significant as Fe-P in the anoxic waters is determined to be low (see results).

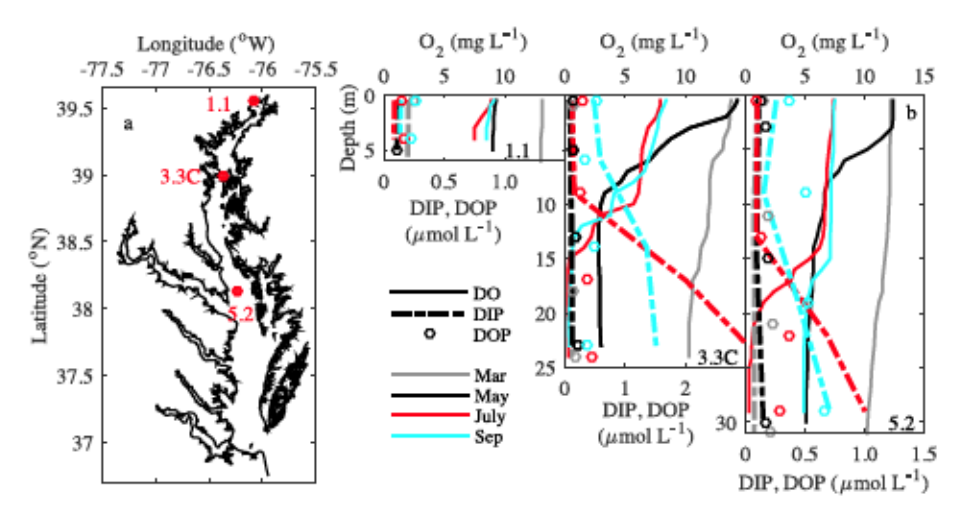


Figure 1. (a) Sampling sites in the Chesapeake Bay (see Table 1 for more details). (b) Vertical distributions of concentrations of dissolved  $O_2$  (mg  $L^{-1}$ ; solid), DIP ( $\mu$ mol  $L^{-1}$ ; dashed), and DOP ( $\mu$ mol  $L^{-1}$ ; circles) in the water column of the Chesapeake Bay. The chemocline is driven by both temperature and salinity gradients (see Figure S1).

## 2.2. Fractionation of P Pools in the Suspended Sediment Particles

Solid-phase partitioning of P pools (both inorganic and organic P, noted as P<sub>i</sub> and P<sub>o</sub> hereafter) in the suspended particles was determined in freeze-dried particle samples following chemical extractions. Particulate inorganic P was fractionated following the sequential sediment extraction (SEDEX) method [Ruttenberg, 1992] into (i) exchangeable or loosely sorbed P (MgCl<sub>2</sub>-P), (ii) ferric Fe-bound P (Fe-P), (iii) authigenic Ca-P (including carbonate fluorapatite, biogenic apatite, and CaCO<sub>3</sub>-bound P), and (iv) detrital apatite P (HCl-P). A fraction of samples were extracted for particulate organic P using 0.25 M NaOH to 0.05 M EDTA solution for 4 h [Cade-Menun, 2005], which likely also extracted P associated with Fe and AI (oxyhyr)oxides [Hupfer et al., 1995]. Concentrations of P<sub>i</sub> and total P (TP; after persulfate digestion) [Gales et al., 1966] in the extract solutions were determined using the molybdenum blue method [Murphy and Riley, 1962]. Concentrations of organic P were determined as the difference between TP and P<sub>i</sub>.

	ampling Locations in the		
Site	Date	Depth (m)	Sampling Depth (m)
1.1	3/20/2014	7.5	S = 0.5  m; B = 6  m
1.1	5/14/2014	6.0	S = 0.5  m; B = 5  m
1.1	7/9/2014	5.5	S = 0.5  m; B = 4  m
1.1	9/17/2014	5.5	S = 0.5  m; B = 4  m
1.1	5/7/2015	6.0	S = 0.5  m; B = 5  m
3.3C	3/19/2014	25.5	S = 0.5  m; $BP = 18  m$ ; $B = 24  m$
3.3C	5/13/2014	24.0	S = 0.5  m; $BP = 13  m$ ; $B = 23  m$
3.3C	7/8/2014	25.0	S = 0.5  m; $BP = 17  m$ ; $B = 24  m$
3.3C	9/16/2014	24.5	S = 0.5  m; $BP = 14  m$ ; $B = 23  m$
3.3C	5/6/2015	25.5	S = 0.5  m; $BP = 16  m$ ; $B = 24  m$
3.3C	7/7/2015	25.0	S = 0.5  m; $AP = 4  m$ ; $BP = 15  m$ ; $AB = 21  m$ ; $B = 24  m$
3.3C	9/15/2015	24.0	S = 0.5  m; $AP = 4  m$ ; $BP = 12  m$ ; $AB = 19  m$ ; $B = 23  m$
5.2	3/19/2014	31.0	S = 0.5  m; $BP = 21  m$ ; $B = 31  m$
5.2	5/12/2014	32,0	S = 0.5  m; BP = 15  m; B = 30  m
5.2	7/7/2014	30.5	S = 0.5  m; BP = 22  m; B = 29  m
5.2	9/15/2014	30.5	S = 0.5  m; $BP = 19  m$ ; $B = 29  m$
5.2	5/5/2015	31.0	S = 0.5  m; BP = 13  m; B = 30  m

<sup>a</sup>Site 1.1 was at the mouth of Susquehanna River (head of the Bay; latitude 39.54667°N, longitude −76.08167°W); Site 3.3C was at north of the Chesapeake Bay Bridge (latitude 38.99583°N, longitude −76.36000°W); Site 5.2 was at the midchannel, close to the mouth of the Potomac River (latitude 38.13667°N, longitude −76.22917°W). Sampling locations (depths (m)) at each station follow the notation of surface (S), above pycnocline (AP), below pycnocline (BP), above bottom (AB), and bottom (B).



### 2.3. Electron Microprobe Analyses

Electron microprobe analyses were conducted on selected samples from site 3.3C (collected in July 2015) to understand the chemical compositions and association of different elements. For this, freeze-dried particulate samples were ground and embedded with epoxy resin, after which cross section of mineral clasts was exposed by cutting and polishing the epoxy assemblage. The samples were carbon coated for conductivity prior to electron microprobe analyses in a JEOL 8530 F electron microprobe at the Pacific Northwest National Laboratory. Energy-dispersive X-ray (EDX) spectroscopy was used for compositional analysis and distribution of key elements including P, Fe, Ca, and Si in particulate samples.

## 2.4. Nuclear Magnetic Resonance (NMR): 1-D 31P and 2-D 1H-31P NMR

Solution <sup>31</sup>P NMR analyses were conducted on the lyophilized NaOH-EDTA extracted solutions to determine the composition of organic P compounds in suspended particles. The NMR spectra were recorded by using an Agilent VNMRS spectrometer operating at 600 MHz in the Environmental Molecular Sciences Laboratory at the Pacific Northwest National Laboratory. Before measurement, samples were redissolved in 1.0 M NaOD and doped with 0.25 mM Gd-DTPA (gadolinium-diethylenetriamine pentaacetic acid) to reduce relaxation delay. A Broad Band X-Observe probe tuned to <sup>31</sup>P was used for the NMR analyses. Other NMR experimental parameters were 90° pulse (18.4 µs), 0.64 s acquisition time, 4s recycle delay, 25°C, and 10,000 scans. The optimum recycle delay (4s) was determined by arraying the recycle delay from 1s to 10s and ensuring that there was no significant change in the intensities of the peaks in the spectrum. It should be noted that addition of relaxation enhancement agent Gd-DTPA significantly reduced T1. Thus, a 4s recycle delay is sufficient for these samples. All recorded spectra were referenced to phosphoric acid at 0 ppm. Data were processed in MestRenova, zero filled to final size of 32,768 points and apodized with 10 Hz line broadening. Phosphorus species and groups were quantified by integrating across chemical shift regions (ppm) corresponding to each group, with region definitions based on *Cade-Menun* [2005]. Regions with integrals less than 0 (due to small baseline errors) were set to 0.

Two-dimensional (2-D) <sup>1</sup>H-<sup>31</sup>P solution NMR analyses were conducted on selected samples to identify the composition of the organic P compounds, using a Bruker Avance III 750 MHz spectrometer with a QXI probe tuned to proton and <sup>31</sup>P. The experimental parameters were 2048 points and 256 points (in the <sup>1</sup>H and <sup>31</sup>P dimensions, respectively), 20°C, 256 scans preincrement, and 2 s recycle delay, with a total acquisition time of about 40 h. The 2-D <sup>1</sup>H-<sup>31</sup>P heteronuclear single quantum correlation (HSQC) spectra were referenced to metaphenylenediamine (MPDA) at 16.92 ppm in the <sup>31</sup>P dimension and 1.86 ppm in the proton dimension, and MPDA chemical shift was referenced in 0.25 M NaOD to phosphoric acid at 0 ppm for <sup>31</sup>P dimension and 4,4-dimethyl-4-silapentane-1-sulfonic acid at 0 ppm for proton dimension. Peak assignments for P compounds were based on the parameters obtained from standard organic P compounds (see supporting information S1 for a list of standard compounds).

## 3. Results

## 3.1. Water Column Oxygen and Dissolved Phosphorus

The water column of the Chesapeake Bay exhibited strong spatial and seasonal variability in physical and geochemical properties. At the northern freshwater site (1.1; 5.5–6.5 m total depth), the water column remained well oxygenated for the entire year (Figures 1b and 2). Total dissolved P (TDP) concentrations remained low for all seasons at site 1.1 (DIP < 0.7  $\mu$ mol L<sup>-1</sup>, and DOP < 0.3  $\mu$ mol L<sup>-1</sup>; Figures 1b and 2). At the deeper middle and south sites (3.3C and 5.2), dissolved oxygen decreased with depth in all seasons (Figure 1b) and was depleted in the bottom waters during summer stratification (Figure 2). Correspondingly, DIP in the summer hypoxic/anoxic water column increased prominently with depth (Figures 1b and 2). As the temperature decreased and stratification weakened in early fall, the water column gradually recovered to the oxic condition and DIP concentrations decreased correspondingly (Figure 2). DOP generally followed a similar seasonal trend, but the increase was less than that of DIP (Figure 2). The dissolved P pool during hypoxic/anoxic seasons was mostly contributed by DIP (DOP contributed 14–20% and 20–30% at sites 3.3C and 5.2, respectively). The timing and extent of summer stratification and hypoxia also exhibited spatial variability (Figure 2, and see Figure S1 for seasonality in vertical distributions of

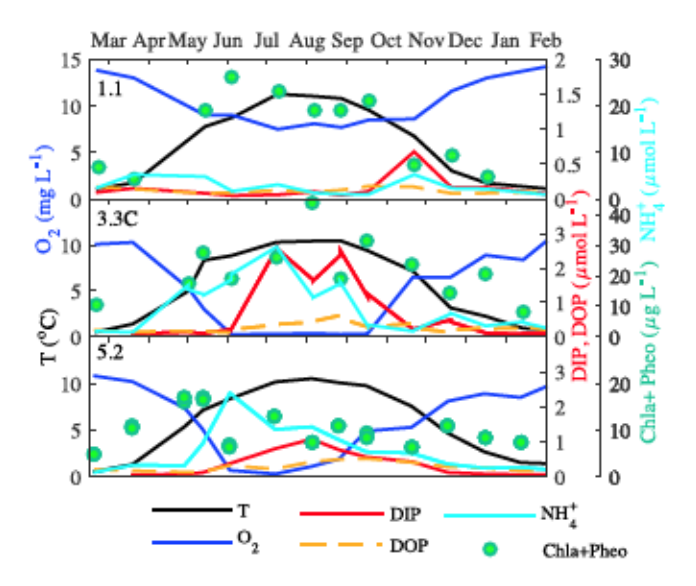


**Figure 2.** Seasonal variability of temperature (°C), chlorophyll a, and pheophylin ( $\mu$ g L $^{-1}$ ) in the surface waters and concentrations of O $_2$  (mg L $^{-1}$ ), DIP ( $\mu$ mol L $^{-1}$ ), DOP ( $\mu$ mol L $^{-1}$ ), and NH $_4$ +( $\mu$ mol L $^{-1}$ ) in the bottom waters.

temperature, salinity, and density): at site 3.3C, hypoxia sustained from early June to mid-September, whereas at site 5.2, the bottom water started to recover in early August.

## 3.2. Composition of P Pools in the Suspended Particles

Concentrations of different P pools in the suspended particles are shown in Tables 2 and 3 and Figures 3 and 4. Concentrations of total particulate phosphorus (PP; µmol L<sup>-1</sup>) generally decreased with depth (Figure 3 and Table 2), with some exceptions in the bottom waters in some seasons likely due to sediment resuspension (e.g., in May 2014, May 2015, and July 2015; Figure 3). When normalized to TSS, concentrations of PP (in µmol g<sup>-1</sup>) showed a clear trend of

decreasing PP with increasing depth (Figure 3 and Table 2). The major inorganic P pools in the suspended particulates are  $MgCl_2$ -P (average  $2.7\pm2.3~\mu mol~g^{-1}$ ), Fe-P (average  $8.2\pm5.8~\mu mol~g^{-1}$ ), and authigenic Ca-P (average  $4.0\pm3.0~\mu mol~g^{-1}$ ). Concentrations of detrital P were relatively low (average  $0.50\pm0.52~\mu mol~g^{-1}$ ). Authigenic Ca-P concentrations generally increased with depth in all seasons (Figure 3). Fe-P concentrations decreased with depth in all seasons at site 3.3C (Figure 3). Detrital Ca-P pools did not show noticeable variability either seasonally or spatially. Total P concentrations in NaOH-EDTA extracted solution ( $TP_{NaOH-EDTA}$ ) ranged from 15 to  $141~\mu mol~g^{-1}$ , contributing > 36% of the PP (Table 3 and Figure 4). Organic P extracted by NaOH-EDTA solution ( $P_{o~NaOH-EDTA}$ ) accounted for  $\sim 4$ –67% of NaOH-EDTA extracted total P ( $TP_{NaOH-EDTA}$ ) and decreased with depth (Table 3).

## 3.3. Electron Microprobe Analyses

EMPA analyses indicated the presence of several minerals, identified by morphology and elemental composition, including some common silicate phases (e.g., quartz, feldspar, mica, and clay), iron sulfides and oxides (e.g., titanomagnetite), and calcium phosphate (Figure 5). The mineral aggregates were generally smaller than  $10\,\mu m$  in diameter, and the individual mineral clasts were usually  $1-2\,\mu m$  across (Figure 5). The identification of a specific mineral, for example, calcium phosphate, was based on numerous measurements of phosphate-bearing clasts, which confirmed that elements other than Ca and P were not consistently and uniformly present in the clasts analyzed. The image and EDX spectrum presented in Figure 5 was representative of an assemblage (<10  $\mu m$  diameter) with a calcium phosphate clast within minute aggregates of other minerals (grains of iron sulfide, titanomagnetite, mica, and silicate).

## 3.4. Solution 1-D <sup>31</sup>P and 2-D <sup>1</sup>H-<sup>31</sup>P NMR Spectroscopy

Solution <sup>31</sup>P NMR spectra of suspended particles at site 3.3C are presented in Figure 6. Inorganic orthophosphate (6 to 7.5 ppm) was present in all samples as one of the most dominant peaks. Other inorganic P forms included pyrophosphate and polyphosphate (peaks at -3 to -5 ppm and -17 to -21 ppm, respectively). Major organic P compounds well resolved from the spectra included orthophosphate monoesters (6 to 2.75 ppm) and diesters (2.75 to -1 ppm). Both monoesters and diesters exhibited multiple pronounced peaks within the integration regions. Peaks in the orthophosphate monoesters region may indicate a wide range of compounds including mononucleotides, components of phospholipids, inositol phosphates, and many other metabolically important sugar phosphates [*Cade-Menun*, 2015]. The multiple peaks in the orthophosphate diester region are most likely contributed by deoxyribonucleic acid and phospholipids [*Cade-Menun*, 2005]. The 2-D <sup>1</sup>H-<sup>31</sup>P HSQC spectra for selected samples are presented in Figure 7, which shows the presence of the specific orthophosphate monoester compounds, including mononucleotides (e.g., 3' Adenosine



Table 2. Total Suspended Solids (TSS), Particulate Phosphorus (PP), and Extractable P (MgCl<sub>2</sub>-P), Ferric Iron Bound P (Fe-P), Authigenic Ca-P (Na Ac-P), and Detrital Ca-P (HCl-P)) in the Water Column of the Chesapeake Bay<sup>a</sup>

				PP					
Site	Time	Depth (m)	TSS ( $\operatorname{mgL}^{-1}$ )	(μg L <sup>-1</sup> )	(μmol g <sup>-1</sup> )	MgCl <sub>2</sub> -P (µmol g <sup>-1</sup> )	Fe-P (μmol g <sup>-1</sup> )	NaAc- P (μmol g <sup>-1</sup> )	HCI- P (μmol g <sup>-1</sup> )
1.1	14 Mar	0.5	13.3	24.8	60.2			0.71	1,2
		6.0	14.7	26.1	57.3			1.4	1.5
	14 May	0.5	8.8	28.4	104.1	2.5	10.0	2.9	0.51
		5.0	10.4	31.3	97.1	2,2	14.8	4.5	0.63
	14 Jul	0.5	4.8	22.0	147.8	2.9	18.0	2.6	0.11
		4.0	5.6	19.6	112,9	1.3	14,7	1.6	0.19
	14 Sep	0.5	6.8	24,2	114.8	2.3	12,5	5.8	1.0
		4.0	6.4	20.4	102.8	2.5	7.8	8.4	2.1
	15 May	0.5	10.8	23.8	71.1	2.0	10.5	7.3	1.6
		5.0	14.8	29.8	65.0	1.3	4.8	7.6	1.4
3.3C	14 Mar	0.5	4.8	16.3	110				
		18	17.6	35.6	65.2			1.3	0.69
		24	25.4	45.8	58.0			6.1	0.70
	14 May	0.5	7.6	21.1	89.6			1.0	0.18
		13	7.2	19.3	86.4	5.9	12.7	3.2	0.27
		23	14	27.0	62.1			1.5	0.68
	14 Jul	0.5	12.8	38.8	97.8			3.9	0.60
		17	7.2	19.7	88.3			8.8	1.7
		24	8.0	15.9	64.4			6.0	1.0
	14 Sep	0.5	10.8	31.2	93.1			0.97	0.15
		14	6.4	8.7	43.8			1.8	0.51
	15.14	23	10.4	12.8	53.0	0.07		2.9	1.3
	15 May	0.5	4.5	12.9	92,4	0.87	6.5	1.7	0.10
		16	4.8 22.5	15.9	107	1.2	3.2	3.1 3.3	0.18
	15 Jul	24 0.5	12.0	34.5	49.5 148	1.1 12.5	1.3	1.8	0.53
	15 Jul	4		55.0			17.8	1.5	0.16
		15	6.4 7.2	23.1 17.7	116 79	3.6	8.0 2.9	3.7	0.10 0.10
		21	7.2	17.7	79	1,4 1,2	2.9	8.8	0.10
		24	55.3	53.8	30.7	1.2	1.7	5.4	0.47
	15 Sep	0.5	6.4	18.0	90.7	2.2	19.9	5.6	0.08
	15 Зер	4.0	5.6	11.2	64.5	3.5	6.6	1.4	0.00
		12	3.2	11.7	117.9	4.0	16.5	5.8	0.06
		19	3.2		117.5	4.8	3.8	15	0.03
		23	3.1	8.6	75.9	1.4	0.10	5.1	0.05
5.2	14 Mar	31	29.6	34.6	38.0		0.10	4.5	0.03
J.2	14 May	0.5	5.7	11.1	63.0	4.4	5.6	0.71	0.05
		15	6.6	11.0	53.8	5.9	3.0	3.8	0.24
		30	22	26.5	38.9	1.2	3.4	4.6	0.26
	14 Jul	0.5	6.2	23.6	124	4.2	3.6	0.2	0.06
		22	3.3	11.0	108	0.34	0	1.4	0.81
	15 May	0.5	6.0	9.1	49.0	1.2		1.9	0.05
		13	15	12.6	27.1	0.83		5.2	0.34
		30	44	35.7	26.2	0.80	2.8	3.8	0.22

<sup>&</sup>lt;sup>a</sup>TSS and PP are from CBP Water Quality Database.

monophosphate (AMP)), the phospholipid components phosphocholine,  $\alpha$ -glycerophosphate and  $\beta$ -glycerophosphate, and the sugar phosphates: glucose-1-phosphate and fructose-1-phosphate. The number and quality of peaks in the 2-D NMR spectra were highest in the samples from March 2014, followed by those from July 2014, and were least for samples from May 2014 (Figure 7).

The concentrations of different P forms calculated from NMR peak integration are shown in Figure 4 and Table 3. In all samples, > 33% of extracted P was inorganic orthophosphate, with its concentration generally increasing with depth and highest concentrations present in July (Table 3). The most dominant organic P compounds were orthophosphate monoesters (~8–43% in surface water), followed by orthophosphate diesters (~2–20% in surface water), pyrophosphate (<14%), and polyphosphate (<5%). Both orthophosphate monoester and diester concentrations decreased with depth (Figure 4). Pyrophosphate concentrations in



Table 3. Concentrations of NaOH-EDTA Extracted Particulate P (TP<sub>NaOH-EDTA</sub>, SRP<sub>NaOH-EDTA</sub>, and P<sub>O-NaOH-EDTA</sub> Represent Total P, SRP, and Organic P; D/M Represents the Diesters to Monoesters Ratio), Authigenic Apatite P (NaAc Solution (pH = 4) Extracted), and Detrital Apatite P (1 M HCl Extracted) in the Water Column of the Chesapeake Bay<sup>a</sup>

			NaOH-EDTA Extracted P									
Site	Time	Depth (m)	TP <sub>NaOH-EDTA</sub> (μmolg <sup>-1</sup> )	SRP <sub>NaOH-EDTA</sub> (μmol g <sup>-1</sup> )	P <sub>o"NaOH-EDTA</sub> (μmol g <sup>-1</sup> )	Monoesters (%)	Diesters (%)	Pyro-P (%)	Poly-P (%)	Orth-P (%)	D/M	Recovery
1.1	14 Mar	0.5			(48.6%)	27.9	7.5	13.2	0	51.4	0.27	
		5.0			(52,4%)	30.0	8.5	13.6	0.3	47.6	0.28	
3.3C	14 Mar	18			(49.3%)	34.7	6.4	6.1	2.1	50.7	0.18	
		24			(52,3%)	40.4	5.1	6.7	0	47.7	0.12	
	14 May	0.5	65.0	29.3	35.8 (55%)	34.3	19.9	0.1	1.0	44.7	0.58	74%
		13			(31%)	20.2	7.8	3.4	0	68.7	0.39	
		23	49.0	39.2	9.8 (20%)	12.8	1.1	5.2	0.5	80.4	0.086	82%
	14 Jul	0.5	114	102	11.3 (10%)	7.9	1.5	0.5	0	90.0	0.19	117%
		17	93.6	86.1	7.5 (8%)	5.4	1.4	0.9	0	92.3	0.25	106%
		24	93.3	89.6	3.7 (4%)	2.5	0.1	1.1	0	96.2	0.04	156%
	14 Sep	0.5	60.0	33.6	26.4 (44%)	36.5	3.9	3.3	0.1	56.2	0.11	65%
	•	14			(16.3%)	12.0	0	4.0	0.3	83.7	0	
		23	54.7	40.5	14.2 (26%)	17.4	0	8.5	0	74.0	0	111%
	15 May	0.5			(45%)	27.3	13.9	3.6	0	55.2	0.51	
		16			(44%)	34.2	6.5	3.0	0	56.2	0.19	
		24	45.8	9.0	36.8 (14%)	9.1- 14.2	1.4	0.8-1.1	0.7	86.4	0.15	89-102%
	15 Jul	0.5	141	66.3	74.7 (53%)	18.4	5.8	7.0	3.9	64.8	0.32	72-96%
		4	73.3	40.1	33.2 (45%)	38.7	5.7	10.4	0.3	44.8	0.15	40-65%
		15	65.3	52.4	13.1 (20%)	14.8	0.1	2.4	0	82.7	0.007	87%
		21	28.3	24.9	2.4 (12%)	3.9	0	5.2	0.5	90.3	0	
		24	20.7	17.1	3.6 (17%)	2.9	0.2	4.6	4.9	87.4	0.069	84%
	15 Sep	4.0	28.2	10.7	17.5 (62%)	43.1	2.1	5	0	49.8	0.049	56%
		19	15.1	7.8	7.1 (47%)	51.2	0	5.2	0.5	48.8	0	
5.2	14 Mar	31			(66.6%)	56.9	8.8	0.9	0	33.4	0.15	

<sup>&</sup>lt;sup>a</sup>Numbers in parentheses for P<sub>o</sub> indicate percentage of P<sub>o</sub> in TP extracted by NaOH-EDTA solution. Recovery was calculated based on the total PP measured (Table 2).

2014 samples showed an increasing trend with depth (Figure 4). However, such a trend was not clear in samples collected in 2015.

#### 4. Discussion

## 4.1. Particulate P Recycling: Organic P Remineralization and Fe-P Remobilization

The strong correlation between dissolved oxygen and P in the Chesapeake Bay water column is characteristic of eutrophic and hypoxic aquatic environments [Kalff, 2001]. During the intensive spring algal bloom (Figure 2), rapid consumption of dissolved oxygen and strengthening of stratification led to bottom hypoxia (Figures 1 and 2). The elevated concentrations of dissolved P (DIP and DOP; Figures 1b and 2) in bottom waters were likely caused by remobilization of particulate P, suggested by the decrease of PP with depth (Figure 3 and Table 2). Assuming that the suspended particles in the surface water represent the most fresh material and the particles in the bottom waters represent those deposited in the surface sediments, P mass balance calculations (Table 4) showed that ~9-50% of the particulate P was recycled into the dissolved P pool (defined as P recycling efficiency (Rp; Table 4 and Figure 8). Rp values were higher at sites 3.3C and 5.2 (averaging 51% and 49%, respectively) compared to Rp values at site 1.1 (average 10%) during 2014-2015. Similarly, a calculation based on 20 years data (1996–2015; Table S2) shows that Rp values at sites 3.3C and 5.2 were statistically higher (F(2, 271) = 78.0, p < 0.001; analyses of variance (ANOVA) in Table S3), likely due to more reactive autochothonous organic matter, longer particle settling time (deeper water), and hypoxic water column thus more Fe-P dissolution. P recycling efficiency was generally higher in the summer (July and September) compared to that of the spring (March and May) (Figure 8 and Table S2; ANOVA in Tables S4-S6). These seasonal variations are expected due to higher metabolic rates (of organic P remineralization) (Figure 2) and reductive dissolution of redox sensitive Fe-P in summer. For example, > 90% of the Fe-P was recycled within the water column at site 3.3C in hypoxic summer (July and September; Table 2).

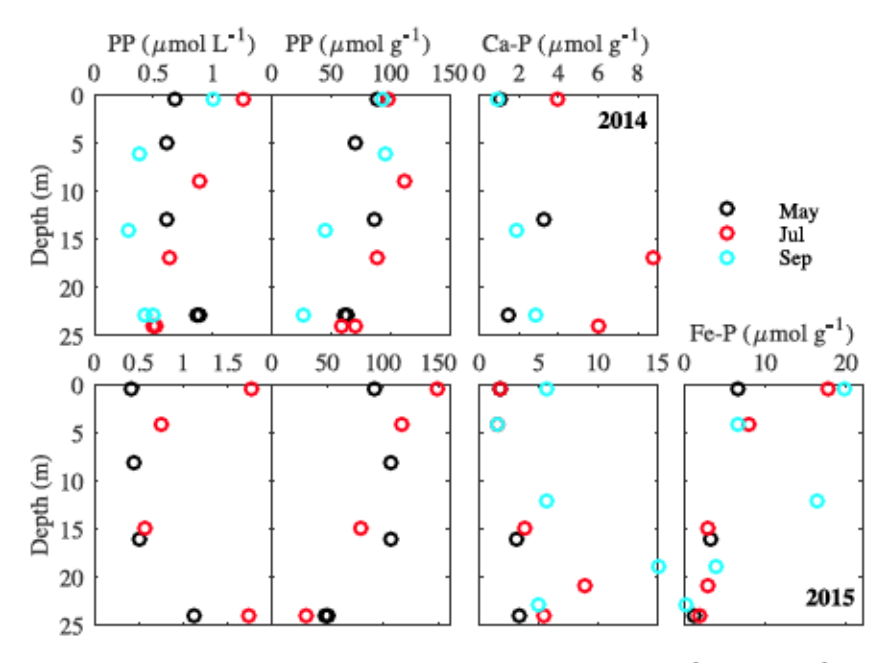


Figure 3. Vertical distributions of P species at site 3.3C: Total particulate P (PP; in μmol L<sup>-1</sup> and μmol g<sup>-1</sup>), authigenic Ca-P (Ca-P; μmol g<sup>-1</sup>), and Fe-P (μmol g<sup>-1</sup>). Data at the top and bottom panels are from 2014 and 2015, respectively.

Remineralization of organic P is essential in supplying bioavailable P in the Chesapeake Bay water column, suggested by the significant decrease of Po with depth (Table 3 and Figure 4). This is also consistent with decrease of particulate carbon and nitrogen, indicating remineralization of organic matter (see Figure S2). In fact, our results show that organic P remineralization is more important than Fe-P remobilization in supplying bioavailable P. Particulate P in the water column in general consists of more organic P than Fe-P (Tables 2 and 3). For example, in July 2015, Fe-P in the surface water at site 3.3C was 17.8 μmol g<sup>-1</sup>, which decreased to 1.7  $\mu$ mol g<sup>-1</sup> (Table 2); the decrease of (17.8–1.7) = 16.1  $\mu$ mol g<sup>-1</sup> in Fe-P was only ~ 23% of the decrease in P<sub>o</sub>

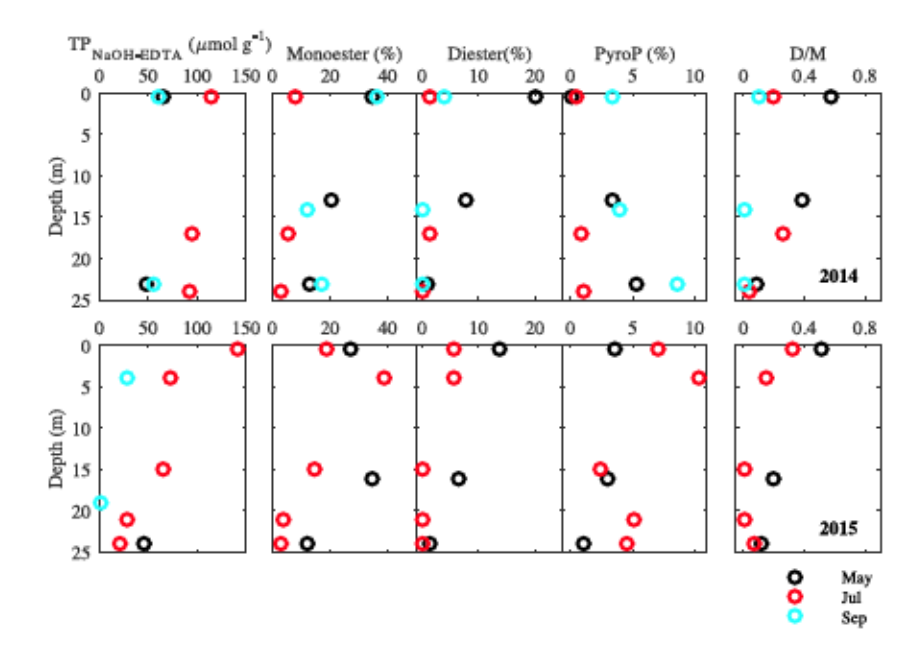
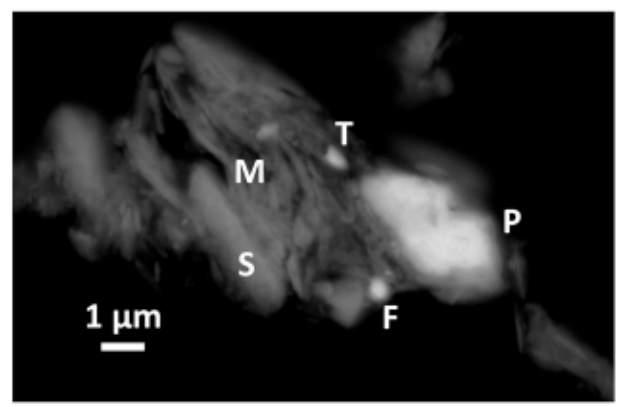
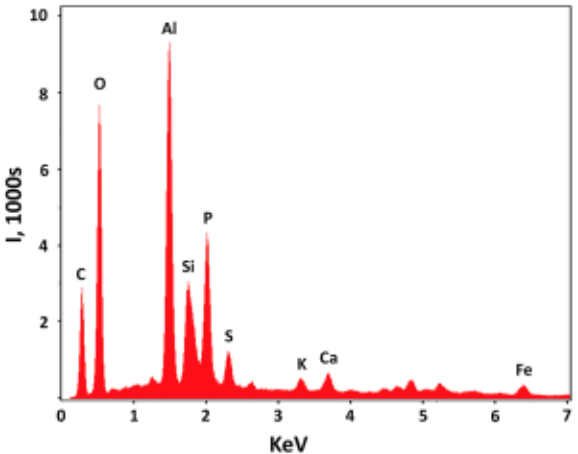


Figure 4. Vertical distributions of NaOH-EDTA extracted P in suspended particles at site 3.3C, including total NaOH-EDTA extracted P (TP<sub>NaOH-EDTA</sub>; µmol g<sup>-1</sup>) and major organic P species (orthophosphate monoester P and orthophosphate diester P, %) and pyrophosphate (%). Data at the top and bottom panels are from 2014 and 2015, respectively.





**Figure 5.** Backscattered electron photomicrograph of a Ca-P-bearing sediment clast. Ca-P (P) associated with other minerals in a micrometer-scale mineral assemblage. The energy-dispersive X-ray spectrum (EDS) from P shows the inclusion of Ca and P; other elements originated from the surrounding material; Ca-P grains generally did not consistently include elements other than Ca and P. T: titanomagnetite; F: iron sulfide; M: mica; S: silicate. Mineral species were deduced from EDS spectra.

((74.7–3.6) = 71.1  $\mu$ mol g<sup>-1</sup>; Table 3). Organic P remineralization in the water column of the Chesapeake Bay likely has been underestimated: particles collected at the surface water may have undergone a certain degree of remineralization, and some of the organic P in the bottom water may be newly produced (benthic production is < 10% of the total primary productivity in the Chesapeake Bay) [Kemp et al., 2005].

Eutrophication in the Chesapeake Bay was caused by increased loadings of nutrients due to anthropogenic alteration of the watershed since the seventeenth century, including land dearance, fertilizer use, and increase of riverine inflow carrying nutrients into the Bay [Boynton et al., 1995; Kemp et al., 2005; Zimmerman and Canuel, 2002]. Development of summer hypoxia in the Bay over the past several decades has increased the vulnerability of the Bay to external P input, as our results suggest that < 10% of the Fe-P reached the sediments as a P sink while the remaining > 90% was recycled within the water column in hypoxic seasons (Table 2). Whereas the external P inputs to the Bay are predominately inorganic (and particulate) forms [Boynton et al., 1995;

Kemp et al., 2005], active biological uptake has transformed P into organic forms that are accumulated and recycled within the system. This is demonstrated by our results showing higher organic P than Fe-P and the dominance of organic P remineralization in sustaining primary productivity. With the dominance of internal P recycling, a projected decrease of nutrient loadings to the Bay [Roberts et al., 2009] may not promise rapid recovery of water quality and reducing eutrophication; rather, it improves water quality in the long term.

## 4.2. Organic Phosphorus Compositions

Orthophosphate monoesters and diesters are the dominant organic P groups in the Chesapeake Bay water column particulates, similar to other marine and freshwater systems [Carman et al., 2000; Paytan et al., 2003; Cade-Menun, 2005; Ahlgren et al., 2006; Cade-Menun et al., 2006]. The multiple peaks in 1-D  $^{31}$ P and 2-D  $^{1}$ H- $^{31}$ P NMR spectra suggest the complex makeup of the monoester and diester groups (Figures 4 and 6). The presence of phosphocholine,  $\alpha$ -glycerophosphate, and  $\beta$ -glycerophosphate (Figure 6) likely resulted from degradation of phospholipids phosphatidylcholine and glycerophospholipids. Seasonal variability in the complexity of the organic P compositions was suggested by the 2-D NMR spectra (Figure 7). The composition of organic P in March 2014 samples was remarkably more complex than that in May 2014 (more peaks in March; Figure 7). This is likely because of the lower temperature in March (Figures 2 and S1), as temperature affects remineralization rates of organic matter (see below). Interestingly, the complexity of particulate organic P compositions increased in July (Figure 7), regardless of the continuing increasing temperature

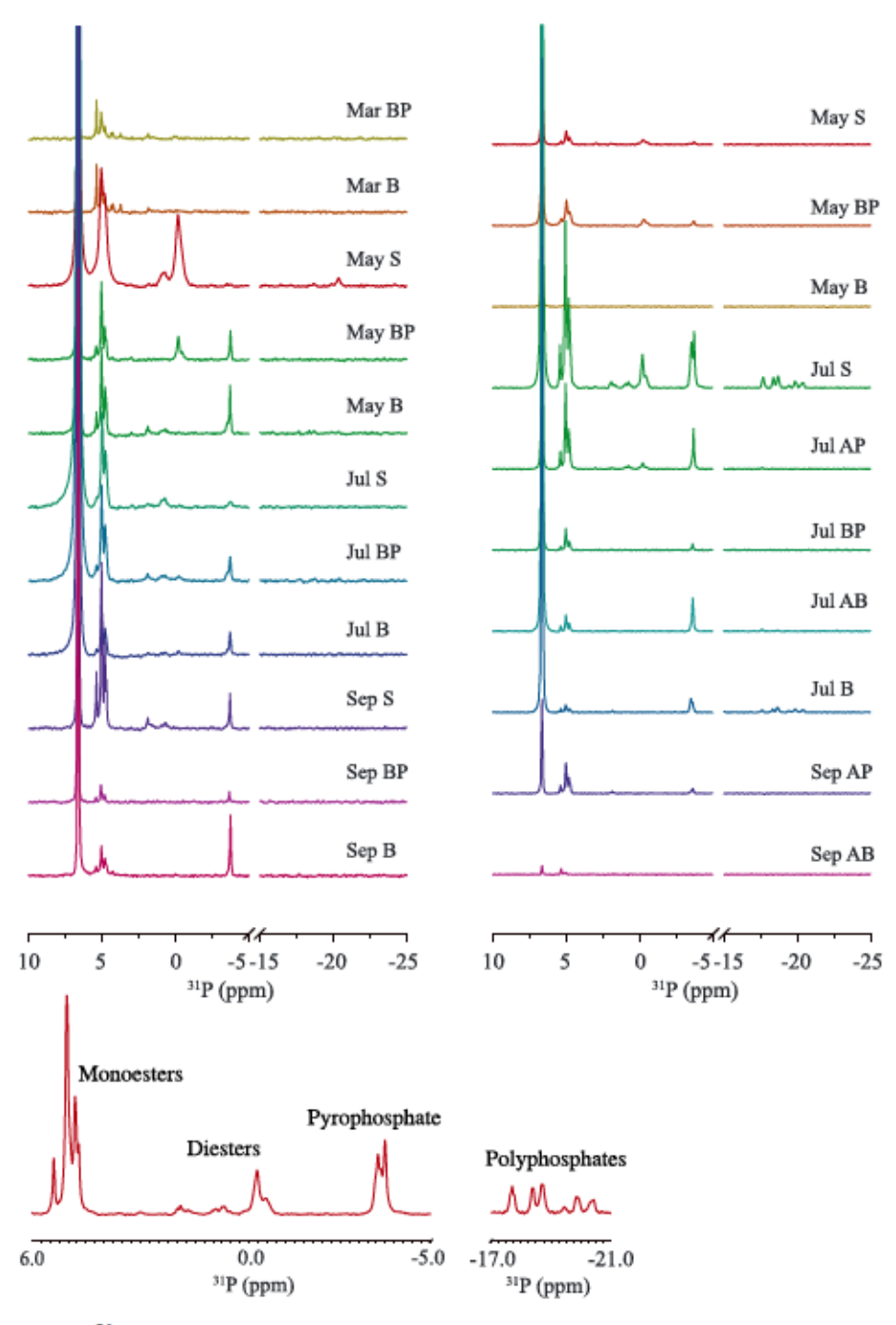


Figure 6. Solution <sup>31</sup>P NMR spectra for particulate organic phosphorus in the water column of the Chesapeake Bay (3.3C). Spectra for samples from (top left) 2014 and (top right) 2015 and (bottom) enlargements of peak regions from one sample (July 2015).

(Figure 1). This is likely due to the effect of anoxic condition developed in late summer (early June to mid-September; Figure 1) and less efficient anaerobic remineralization of relatively refractory organic matters (see below).

### 4.3. Organic P Transformations and Diester-to-Monoester (D/M) Ratios

Remineralization of settling organic debris in the water column was indicated by decrease of both orthophosphate monoesters and diesters with depth. Caution is needed for quantitative interpretation of these results because transformation may occur during sample processing: rapid degradation of RNA (an orthophosphate

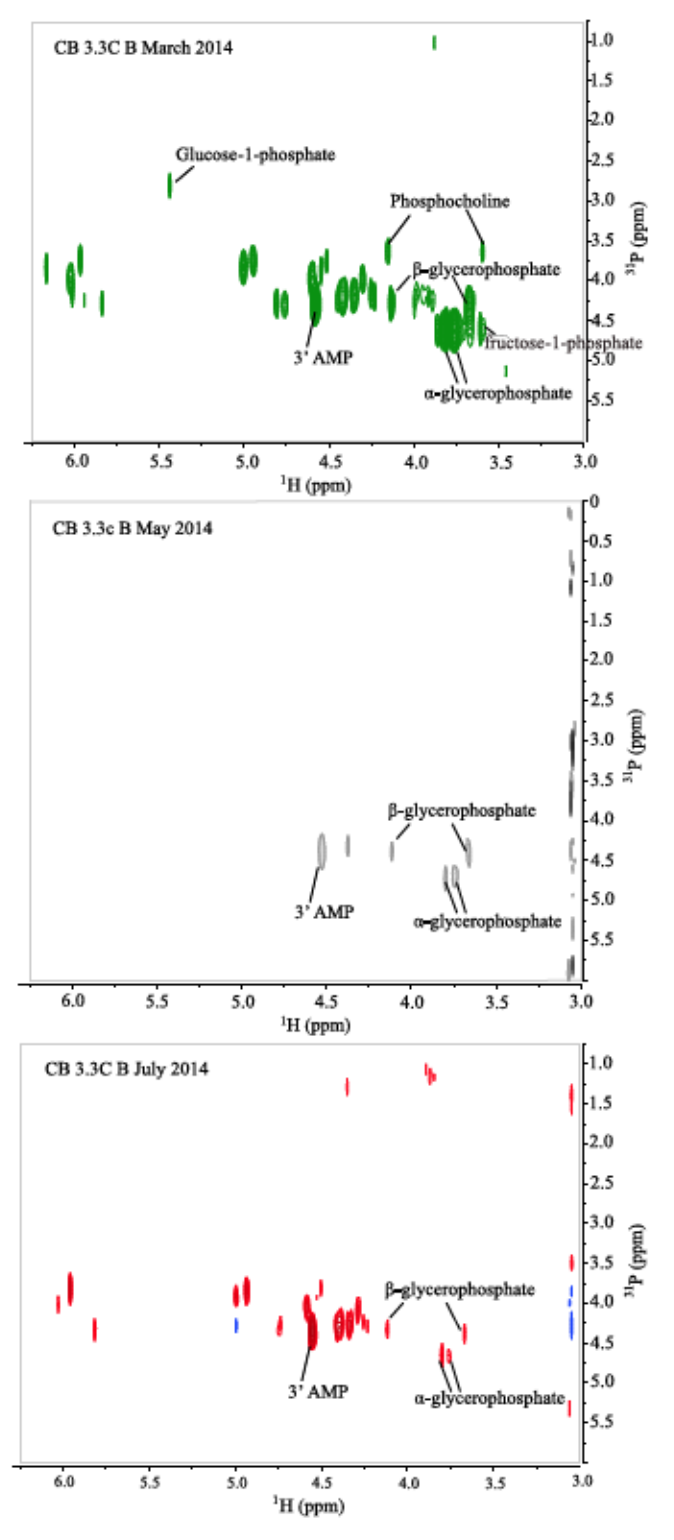


Figure 7. The 2-D <sup>1</sup>H-<sup>31</sup>P HSQC spectra for particulate organic phosphorus in the water column of the Chesapeake Bay.

diester) during the extraction [Makarov et al., 2002] may lead to underestimation of orthophosphate diesters and overestimation of orthophosphate monoesters. Interestingly, relatively low percentages of both esters in surface water were found in July (Figure 4), which may indicate intensive remineralization of organic matter at the surface water. The diester-to-monoester (D/M) ratios can be used as an indicator of the degree of organic matter remineralization: a lower D/M ratio suggests higher degree of remineralization, because orthophosphate diesters are more labile than monoesters [Paytan et al., 2003; Ahlgren et al., 2006] and diester degradation generates monoesters. The D/M ratios of the suspended particles at site 3.3C generally decreased with depth in all seasons (Figure 4 and Table 3), consistent with organic P degradation. The D/M ratios were also lower in July and September compared to those in May (Figure 4). Assuming that contributions from degradation of RNA to orthophosphate monoesters during extraction are similar between different seasons, the low D/M ratios in July and September may suggest enhanced remineralization of organic P at high temperature in summer.

Changes in redox conditions over the summer and early fall (May-Sep) may also impact organic P remineralization and D/M ratios. A previous study has suggested less efficient degradation of diesters in anoxic sediment [Carman et al., 2000]. If this is also true in the water column, our results (lower D/M ratios in anoxic water column) may suggest that the oxic/anoxic conditions have a stronger effect on degradation of monoesters compared to that of diesters. In other words, the difference between degradation rates of diester and

monoester may be even larger under anaerobic conditions. It was suggested that less effective remineralization of relatively refractory organic matter occurs under anoxic versus oxic conditions, while labile organic matter is less oxygen sensitive [Burdige, 2007, and references therein]. Our results are consistent with the

Table 4.	Recycling Efficiency of Particulate Organic P ( $R_P$ ; %) in the Water Column of the Chesapeake Bay <sup>a</sup> Recycling Efficiency								
Time	1.1	3.3C	5.2						
14 Mar	4.8%	45.7%	25.3%						
14 May	6.7%	31.8%	56.6%						
14 Jul	23.6%	59.0%; 46.9%	53.4%; 20.2%						
14 Sep	15.7%; 10.4%	58.8%; 44.7%	63.7%						
15 May	8.6%	52.8%	59.1%						
15 Jul	2.1%	79.3%	67.9%; 62.0%						
Average	$9.4 \pm 6.4\%$ (21.5 ± 15.5%)	50.2 ± 14.5% (51.6 ± 17.7%)	47.8 ± 17.9% (51.0 ± 20.4%)						

<sup>a</sup>Remineralization efficiency ( $R_P$ ) was calculated as ( $PP_S - PP_B$ )/ $PP_S \times 100\%$ , where  $PP_S$  and  $PP_B$  stand for concentrations of particulate P (mg L<sup>-1</sup>) in surface (or depth with maximum PP) and bottom water, respectively (see Tables 2 and S1 for PP and TSS). When the bottom water experienced strong sediment suspension (e.g., in 14 March) and P concentrations (as mass per volume water) were strongly affected by increase of sediment mass in the bottom waters (see TSS in Table 2), PP concentrations as mass per sediment mass (in  $\mu$  mol  $g^{-1}$ ) were used for the calculation of  $R_P$  (in dicated as underlined numbers). For consistency and easy comparison among sites the average values were calculated using the underlined numbers. Twenty years of historical data (from 1996 to 2015) were also used to calculate P recycling efficiencies; the average and standard deviation for each site are given in parentheses (also see Figure 8 and Table S2). This calculation using PP concentrations as mass per sediment mass (in  $\mu$  mol  $g^{-1}$ ) underestimates the remineralization efficiency, as the decrease of sediment P should account for both the decrease of P concentration in sediments  $(\mu mol g^{-1})$  and the decrease of sediment content in water (TSS;  $mgL^{-1}$ ) (see comparison of results from the two different calculations, at 1.1 (14 September), 3.3C (14 July and 14 September), and 5.2 (14 and 15 July).

selective concentration of less labile fractions observed under anoxic conditions [Burdige, 2007]. However, caution must be taken when comparing our results in the water column to those in sediments [e.g., Carman et al., 2000], where organic P may less reactive. Degradation of organic P and of bulk organic matter (including C and N) may also be different. Variability in D/M ratios may also be a result of changing biological communities. Nevertheless, the D/M ratios could be a useful proxy for understanding the composition and remineralization of organic P, suggesting strong seasonal and spatial variability in organic P transformation in the water column of the bay.

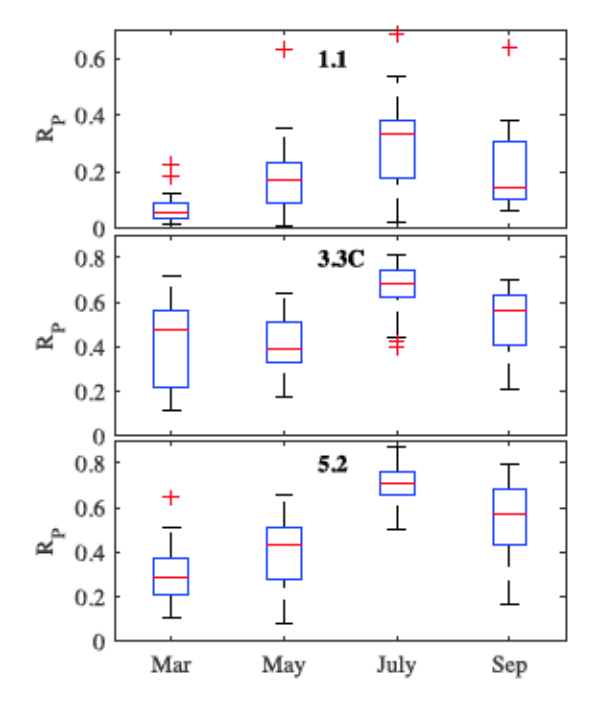


Figure 8. P recycling efficiency (Rp) in the water column of the Chesapeake Bay (plotted for data from 1996–2015). The red line marks the median value; bottom and top of the box marks the 25th and 75th percentiles for the data set (i.e., 25% and 75% of the values are below); height of the box represents the interquartile range (IQR); ends of the whiskers mark the highest and lowest values of the data set that are within 1.5 times the IQR; outliers are beyond 1.5 IQR).

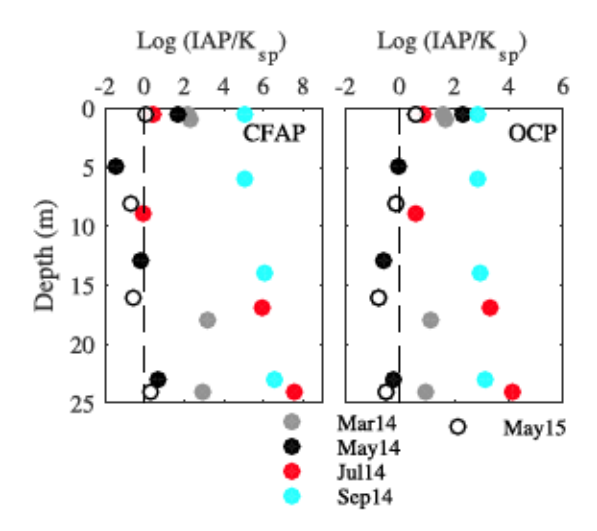


Figure 9. Saturation states of carbon fluorapatite (CFAP) and octacalcium phosphate (OCP) in the water column of the Chesapeake Bay.

#### 4.4. Pyrophosphate and Polyphosphate

Increased pyrophosphate concentration with depth in 2014 (Figure 4 and Table 3) may suggest rapid degradation of polyphosphates and/or other energy storage compound (such as ADP and ATP), as pyrophosphate itself can be rapidly degraded [Ahlgren et al., 2005]. The high concentrations of polyphosphate in the anoxic water column in July 2015 are interesting. It is suggested that polyphosphate may be redox sensitive and can be degraded rapidly in anoxic sediments [Carman et al., 2000; Cade-Menun et al., 2006; Hupfer and Rübe, 2004; Diaz et al., 2012]. We hypothesize that in the Chesapeake Bay, polyphosphate may have been produced in the aerobic surface waters and subsequently settled down to anoxic water and reached the bottom before being fully degraded within the water column (<25 m at site 3.3C). Biological synthesis of polyphosphate likely occurs in the summer when DIP concentrations in the anoxic/hypoxic waters are high, resulting in an increased P flux to the surface water and "luxury" P uptake [Khoshmanesh et al., 2002; Martin and Van Mooy, 2013]. The high production of poly-P in the surface water in summer and its subsequent degradation in the deeper anoxic waters (also suggested by the higher pyrophosphate) may provide a second positive feedback for P recycling in the Bay besides the dassical Fe-P coupling, although further quantitative investigation is needed for understanding its importance in the bay.

## 4.5. Authigenic Calcium Phosphate in the Water Column

The high concentrations of NaAc extractable P, a common indicator for authigenic carbonate fluorapatite (CFAP) in marine sediments [Ruttenberg, 1992; Ruttenberg and Berner, 1993], may suggest the presence of authigenic Ca-P in the water column of the Chesapeake Bay. EMPA also suggests the presence of discrete Ca-P grains (Figure 5). Although EMPA cannot discriminate authigenic Ca-P (precipitated in the water column) from exported Ca-P (e.g., dust deposition) [Eijsink et al., 2000], the increase of Ca-P concentrations with depth (Figure 3) may suggest in situ precipitation or mineral growth while settling. While contributions from resuspended sediments cannot be excluded, the seasonal trends of sediment resuspension (high in March and May) were inconsistent with the trends of Ca-P (high in July). In contrast, the similar trends of DIP and Ca-P (Figures 1 and 3) suggest Ca-P precipitation due to saturation. Thermodynamic calculations (see S2) suggest that the water was supersaturated with CFAP and its precursor octacalcium phosphate (OCP) [Atlas, 1975; Gunnars et al., 2004] (Figure 9). The trends in Ca-P saturation index (Figure 9) are also consistent with the increasing Ca-P and the decreasing particulate P concentrations with depth (Figure 2 and Tables 2 and 3), indicative of Ca-P precipitation at the expense of other forms of PP (e.g., organic P). Formation of authigenic Ca-P in sinking particulate from other forms of P was also suggested by recent studies in marine environments [Faul et al., 2005; Lyons et al., 2011].

CFAP mineral is commonly formed in many marine sediments as an important long-term P sink [e.g., Jahnke et al., 1983; Ruttenberg and Berner, 1993]; however, its precipitation in water column is rarely reported.



Concentration of Ca-P in the water column is comparable to that in sediments (3-5 µmol g<sup>-1</sup> at mesohaline sites), which constitutes ~ 40% of the long-term P sink as sediment burial (with the remaining 60% attributed to Fe-P burial) [Joshi et al., 2015], Precipitation of CFAP in seawater is hindered by the low phosphate concentrations [Martens and Harriss, 1970] and the slow kinetics of nucleation [Martens and Harriss, 1970; Atlas and Pytkowicz, 1977; Van Cappellen and Berner, 1991]. In the hypoxic waters of the Chesapeake Bay, precipitation of CFAP is thermodynamically favored due to the high phosphate concentrations. Nucleation may be facilitated by formation of Ca-P precursors (e.g., OCP forms within several days) [Atlas, 1975], while recrystallization into apatite can occur in sediments on longer time scales [Gunnars et al., 2004; Oxmann and Schwendenmann, 2014, 2015]. It was also suggested that polyphosphate may serve as a template for apatite nucleation [Diaz et al., 2008]: in the Chesapeake Bay the high concentrations of polyphosphate in July also coincided with the high Ca-P concentrations. Further rigorous investigation is needed for the possibility and mechanisms of authigenic Ca-P precipitation and its contribution to P sequestration in the Bay (Table 4).

## 5. Conclusions and Implications

Our findings on the compositions and transformations of particulate P in the water column provide several insights into the P cycling in the Chesapeake Bay. First, remineralization of organic P is the dominant contributor for resupplying dissolved P into the water column of the Chesapeake Bay rather than remobilization of Fe-P. This suggests that internal P cycling is more important in sustaining the primary productivity in the short term (e.g., in seasonal time scale) compared to the external P input. Therefore, nutrient management to reduce watershed P inputs may not improve the water quality rapidly. However, such efforts could help reduce eutrophication in the long term; due to the effective Fe-P remobilization in hypoxic waters, acceleration of eutrophication likely occurs if P loadings increase. Second, our results highlight the complexity of the feedback mechanisms between hypoxia and eutrophication: while the extent of hypoxia/anoxic in the bottom waters regulates P immobilization as anoxic, conditions in summer and early fall are favorable for Fe-P dissolution; more efficient remineralization of particulate organic P, which constitutes a much larger fraction of the sinking particulate P, occurs in oxic rather than anoxic conditions. Precipitation of Ca-P in the water column as a P sink promoted by high P concentrations in the hypoxic waters may also decrease recycled P. On the other hand, polyphosphate cycling (synthesis and degradation) in the hypoxic water column may provide another positive feedback mechanism besides the Fe-P coupling.

## **Acknowledgments**

We thank Debbie McKay, Kristen Heyer, Laura Fabian, and others at the Maryland Department of Natural Resources and Captain Rick Younger and the crew of R/V Kerhin for help with sample acquisition. We acknowledge Lisa Stout, Ha Vu, Nirman Dhakal, Mingjing Sun, Dengjun Wang, Huj Li, Qiang Li, and Balakrishna Avula for help with collection and preprocessing water samples. Nancy Washton is acknowledged for discussions on NMR methods. The work was supported by grants from the U.S. Department of Agriculture (2015-67020 and 2016-08499) and the National Science Foundation (1301765) and 1654642). A portion of the research was performed using EMSL, a DOE Office of Science User Facility sponsored by the Office of Biological and Environmental Research located at Pacific Northwest National Laboratory (EMSL proposal 48437). We are thankful to the Chesapeake Bay Program for sharing the water column geochemistry data, which can be obtained freely from the CBP Data Hub (http://www.chesapeakebay.net/data). Supporting data are included as tables in the supporting information; any additional data can be obtained from J.L. (e-mail: lijiying@udel. edu). We thank reviewers for their constructive comments that helped improve the quality of the manuscript.

### References

Ahlgren, J., L. Tranvik, A. Gogoll, M. Waldeback, K. Markides, and E. Rydin (2005), Sediment depth attenuation of biogenic phosphorus compounds measured by P-31 NMR, Environ. Sci. Technol., 39(3), 867-872.

Ahlgren, J., K. Reitzel, L. Tranvik, A. Gogoll, and E. Rydin (2006), Degradation of organic phosphorus compounds in anoxic Baltic Sea sediments: A P-31 nuclear magnetic resonance study, Limnol. Oceanogr., 51(5), 2341-2348.

Aspila, K. I., H. Agemian, and A. S. Y. Chau (1976), Semiautomated method for determination of inorganic, organic and total phosphate in sediments, Analyst, 101(1200), 187-197.

Atlas, E., and R. M. Pytkowicz (1977), Solubility behavior of apatites in seawater, Limnol. Oceanogr., 22(2), 290-300.

Atlas E. L. (1975), Phosphate equilibria in seawater and interstitial waters, PhD thesis, Ore. State Univ., Corvallis.

Ator, S. W., and J. M. Denver (2015), Understanding nutrients in the Chesapeake Bay watershed and implications for management and restoration—The eastern shore, U.S. Geol. Surv. Circ., 1406, 72.

Biggs, R. B. (1970), Sources and distribution of suspended sediment in northern Chesapeake Bay, Mar. Geol., 9(3), 187-210.

Boynton, W. R., and W. M. Kemp (1985), Nutrient regeneration and oxygen-consumption by sediments along an estuarine salinity gradient, Mar. Ecol. Prog. Ser., 23(1), 45-55.

Boynton, W. R., J. H. Garber, R. Summers, and W. M. Kemp (1995), Inputs, transformation, and transport of nitrogen and phosphorus in Chesapeake Bay and selected tributaries, Estuaries, 18(1B), 285-314.

Boynton, W. R., and E. M. Balley (2008), Sediment Oxygen and Nutrient Exchange Measurements From Chesapeake Bay, Tributary Rivers and Maryland Coastal Bays: Development of a Comprehensive Database and Analysis of Factors Controlling Patterns and Magnitude of Sediment-Water Exchanges, 202 pp., Univ. of Md. Cent. for Environ. I Sci., Solomons.

Burdige, D. J. (2007), Preservation of organic matter in marine sediments: Controls, mechanisms, and an imbalance in sediment organic carbon budgets?, Chem. Rev., 107(2), 467-485.

Cade-Menun, B. J. (2005), Characterizing phosphorus in environmental and agricultural samples by P-31 nuclear magnetic resonance spectroscopy, Talanta, 66(2), 359-371.

Cade-Menun, B. J. (2015), Improved peak identification in P-31-NMR spectra of environmental samples with a standardized method and peak library, Geoderma, 257, 102-114.

Cade-Menun, B. J., J. A. Navaratnam, and M. R. Walbridge (2006), Characterizing dissolved and particulate phosphorus in water with P-31 nuclear magnetic resonance spectroscopy, Environ, Sci. Technol., 40(24), 7874-7880.

Carman, R., G. Edlund, and C. Damberg (2000), Distribution of organic and inorganic phosphorus compounds in marine and lacustrine sediments: A P-31 NMR study, Chem. Geol., 163(1-4), 101-114.

- Chesapeake Bay Program (2012), Guide to using Chesapeake Bay program water quality monitoring data, United States Environmental Protection Agency, Annapolis, [Available at http://www.chesapeakebay.net/documents/3676/wg\_data\_userquide\_10feb12\_mod.pdf]
- Chesapeake Bay Program (2016), Chesapeake Bay program water quality database 1984-present. [Available at http://www.chesapeakebay. net/data/downloads/cbp\_water\_quality\_database\_1984\_present.]
- Conley, D. J., W. M. Smith, J. C. Cornwell, and T. R. Fisher (1995), Transformation of particle-bound phosphorus at the land-sea interface, Estuarine Coastal Shelf Sci., 40, 161-176.
- Comwell, J. C., D. J. Conley, M. Owens, and J. C. Stevenson (1996), A sediment chronology of the eutrophication of Chesapeake Bay, Estuaries, 19(2B), 488-499.
- Cowan, J. L. W., and W. R. Boynton (1996), Sediment-water oxygen and nutrient exchanges along the longitudinal axis of Chesapeake Bay: Seasonal patterns, controlling factors and ecological significance, Estuaries, 19(3), 562-580.
- Diaz, J., E. Ingall, C. Benitez-Nelson, D. Paterson, M. D. de Jonge, I. McNulty, and J. A. Brandes (2008), Marine polyphosphate: A key player in geologic phosphorus sequestration, Science, 320(5876), 652-655.
- Diaz, J. M., E. D. Ingall, S. D. Snow, C. R. Benitez-Nelson, M. Taillefert, and J. A. Brandes (2012), Potential role of inorganic polyphosphate in the cycling of phosphorus within the hypoxic water column of Effingham Inlet, British Columbia, Global Biogeochem. Cycles, 26, GB2040, doi:10.1029/2011GB004226.
- Eijsink, L. M., M. D. Krom, and B. Herut (2000), Speciation and burial flux of phosphorus in the surface sediments of the Eastern Mediterranean, Am. J. Sci., 300(6), 483-503.
- Faul, K. L., A. Paytan, and M. L. Delaney (2005), Phosphorus distribution in sinking oceanic particulate matter, Mar. Chem., 97(3-4), 307-333. Fisher, T. R., A. B. Gustafson, K. Sellner, R. Lacouture, L. W. Haas, R. L. Wetzel, R. Magnien, D. Everitt, B. Michaels, and R. Karrh (1999), Spatial and temporal variation of resource limitation in Chesapeake Bay, Mar. Biol., 133(4), 763-778.
- Fitzsimons, M. F., M. C. Lohan, A. D. Tappin, and G. E. Millward (2012), The role of suspended particles in estuarine and coastal biogeochemistry, in Geochemistry of Estuaries and Coasts, vol. 4, pp. 71–114, Elsevier, Amsterdam, Netherlands.
- Gales, M. E., E. C. Julian, and R. C. Kroner (1966), Method for quantitative determination of total phosphorus in water, J. Am. Water Works Assoc., 58(10), 1363-1368.
- Gunnars, A., S. Blomqvist, and C. Martinsson (2004), Inorganic formation of apatite in brackish seawater from the Baltic Sea: An experimental approach, Mar. Chem., 91(1-4), 15-26.
- Hagy, J. D., W. R. Boynton, C. W. Keefe, and K. V. Wood (2004). Hypoxia in Chesapeake Bay, 1950-2001: Long-term change in relation to nutrient loading and river flow, Estuaries, 27(4), 634-658.
- Hecky, R. E., and P. Kilham (1988), Nutrient limitation of phytoplankton in fresh-water and marine environments—A review of recentevidence on the effects of enrichment, Limnol. Oceanogr., 33(4), 796-822.
- Hupfer, M., and B. Rübe (2004), Origin and diagenesis of polyphosphate in lake sediments: A 31P-NMR study, Limnol. Oceanogr., 49(1),
- Hupfer, M., R. Gächter, and R. Giovanoli (1995), Transformation of phosphorus species in settling seston and during early sediment diagenesis, Aquat, Sci., 57(4), 305-324.
- Hyacinthe, C., and P. Van Cappellen (2004). An authigenic iron phosphate phase in estuarine sediments: Composition, formation and chemical reactivity, Mar. Chem., 91(1-4), 227-251.
- Jahnke, R. A., S. R. Emerson, K. K. Roe, and W. C. Burnett (1983), The present-day formation of apatite in Mexican continental-margin sediments, Geochim. Cosmochim. Acta, 47(2), 259-266.
- Jilbert, T., and C. P. Slomp (2013), Iron and manganese shuttles control the formation of authigenic phosphorus minerals in the euxinic basins of the Baltic Sea, Geochim, Cosmochim, Acta, 107, 155-169.
- Joshi, S. R., R. K. Kukkadapu, D. J. Burdige, M. E. Bowden, D. L. Sparks, and D. P. Jaisi (2015), Organic matter remineralization predominates phosphorus cycling in the mid-bay sediments in the Chesapeake Bay, Environ. Sci. Technol., 49(10), 5887-5896.
- Kalff, J. (2001), Limnology: Inland Water Ecosystems, Prentice Hall, Upper Saddle River, N. J.
- Karl, D. M. (2014), Microbially medicated transformations of phosphorus in the sea: New views of an old cycle, Ann. Rev. Mar. Sci., 6, 279–337. Keefe, C. W. (1994), The contribution of inorganic-compounds to the particulate carbon, nitrogen, and phosphorus in suspended matter and surface sediments of Chesapeake Bay, Estuaries, 17(1B), 122-130.
- Kemp, W. M., et al. (2005), Eutrophication of Chesapeake Bay: Historical trends and ecological interactions, Mar. Ecol. Prog. Ser., 303, 1-29. Khoshmanesh, A., B. T. Hart, A. Duncan, and R. Beckett (2002), Luxury uptake of phosphorus by sediment bacteria, Water Res., 36(3), 774-778. Lyons, G., C. R. Benitez-Nelson, and R. C. Thunell (2011), Phosphorus composition of sinking particles in the Guaymas Basin, Gulf of California, Limnol. Oceanogr., 56(3), 1093-1105.
- Makarov, M. I., L. Haumaier, and W. Zech (2002), Nature of soil organic phosphorus: An assessment of peak assignments in the diester region of P-31 NMR spectra, Soil Biol. Biochem., 34(10), 1467-1477.
- Martens, C. S., and R. C. Harriss (1970), Inhibition of apatite precipitation in marine environment by magnesium ions, Geochim. Cosmochim. Acta, 34(5), 621-625.
- Martin, P., and B. A. S. Van Mooy (2013), Fluorometric quantification of polyphosphate in environmental plankton samples: Extraction protocols, matrix effects, and nucleic acid interference, Appl. Environ. Microbiol., 79(1), 273-281.
- Murphy, J., and J. P. Riley (1962), A modified single solution method for the determination of phosphate in natural waters, Anal. Chim. Acta, 27, 31-36.
- Oxmann, J. F., and L. Schwendenmann (2014), Quantification of octacalcium phosphate, authigenic apatite and detrital apatite in coastal sediments using differential dissolution and standard addition, Ocean Sci., 10(3), 571-585.
- Oxmann, J. F., and L. Schwendenmann (2015), Authigenic apatite and octacalcium phosphate formation due to adsorption-precipitation switching across estuarine salinity gradients, Biogeosciences, 12(3), 723-738.
- Paytan, A., B. J. Cade-Menun, K. McLaughlin, and K. L. Faul (2003), Selective phosphorus regeneration of sinking marine particles: Evidence from P-31-NMR, Mar. Chem., 82(1-2), 55-70.
- Prasad, M. B. K., M. R. P. Sapiano, C. R. Anderson, W. Long, and R. Murtugudde (2010), Long-term variability of nutrients and chlorophyll in the Chesapeake Bay: A retrospective analysis, 1985–2008, Estuaries Coasts, 33(5), 1128–1143.
- Read, E. K., M. Ivancic, P. Hanson, B. J. Cade-Menun, and K. D. McMahon (2014), Phosphorus speciation in a eutrophic lake by P-31 NMR spectroscopy, Water Res., 62, 229-240.
- Roberts, A. D., S.D. Prince, C. A. Jantz, and S. J. Goetz (2009), Effects of projected future urban land over on nitrogen and phosphorus runoff to Chesapeake Bay, Ecol. Eng., 35, 1758-1722.
- Ruttenberg, K. C. (1992), Development of a sequential extraction method for different forms of phosphorus in marine-sediments, Limnol. Oceanogr., 37(7), 1460-1482.



- Ruttenberg, K. C., and R. A. Berner (1993), Authigenic apatite formation and burial in sediments from non-upwelling, continental-margin environments, *Geochim. Cosmochim. Acta*, 57(5), 991–1007.
- Sannigrahi, P., and E. Ingall (2005), Polyphosphates as a source of enhanced P fluxes in marine sediments overlain by anoxic waters: Evidence from P-31 NMR, Geochem. Trans., 6(3), 52–59.
- Schenau, S., C. P. Slomp, and G. J. DeLange (2000), Phosphogenesis and active phosphorite formation in sediments from the Arabian Sea oxygen minimum zone, Mar. Geol., 169(1-2), 1-20.
- Sekula-Wood, E., C. R. Benitez-Nelson, M. A. Bennett, and R. Thunell (2012), Magnitude and composition of sinking particulate phosphorus fluxes in Santa Barbara Basin, California, Global Biogeochem. Cycles, 26, GB2023, doi:10.1029/2011GB004180.
- van Cappellen, P., and R. A. Berner (1991), Fluorapatite crystal-growth from modified seawater solutions, Geochim. Cosmochim. Acta, 55(5), 1219–1234.
- Wang, H., A. Appan, and J. S. Gulliver (2003), Modeling of phosphorus dynamics in aquatic sediments: II—Examination of model performance, Water Res., 37, 3939–3953.
- Zhang, X., M. Roman, D. Kimmel, C. McGilliard, and W. Boicourt (2006), Spatial variability in plankton biomass and hydrographic variables along an axial transect in Chesapeake Bay, J. Geophys. Res., 111, C05511, doi:10.1029/2005JC003085.
- Zimmerman, A. R., and E. A. Canuel (2002), Sediment geochemical records of eutrophication in the mesohaline Chesapeake Bay, Limnol. Oceanogr., 47(4), 1084–1093.